



## CLEAVAGE FRACTURE OF WARM BRACKISH ICE

J.P. Dempsey<sup>1</sup>, P. Jochmann<sup>2</sup>, L. Fransson<sup>3</sup>, Z. Mu<sup>4</sup>, J. Weiss<sup>5</sup>, A.C. Palmer<sup>6</sup>

<sup>1</sup>Clarkson University, Potsdam, New York, USA

<sup>2</sup>Hamburg Ship Model Basin, Hamburg, GERMANY

<sup>3</sup>Luleå University of Technology, Luleå, SWEDEN

<sup>4</sup>MMI Engineering, Houston, Texas, USA

<sup>5</sup>CNRS, LGGE, Saint-Martin d'Hères, FRANCE

<sup>6</sup>National University of Singapore, SINGAPORE

### ABSTRACT

Two sets of cleavage (cracking parallel to the ice surface) fracture toughness tests were conducted at the Hamburg Ship Model Basin (HSVA) on brackish ice harvested from two separate locations in the Gulf of Bothnia. The ice was split using a pin-loaded compact tension geometry. The fracture tests were accompanied by tensile and compressive tests. This paper discusses the experiments and the results.

### INTRODUCTION

The cleavage cracking orientation is shown in Figure 1; the planar crack nucleates and propagates parallel to the ice surface. This ice mechanics terminology was apparently first used by Schwarz et al., 1974. Parsons et al. (1986) defined this orientation as “horizontal orientation, horizontal propagation” or HH. Cleavage cracking during ice-structure indentation has been discussed sporadically since the early seventies (further references may be gleaned from Evans et al., 1984; Kärnä and Järvinen, 1999). With the advent of the indentation tests sponsored by the Japan Ocean Industry Association (JOIA), the importance of the cleavage cracking mode of failure in ice-structure interactions has become firmly established (Matsushita et al., 2000, 2001). JOIA recently sponsored cleavage fracture and cleavage-related strength tests on the Okhotsk sea ice (Kamio et al., 2003). This paper investigates the cleavage fracture toughness and the cleavage-related compressive-tensile strength of the brackish ice in the Gulf of Bothnia.

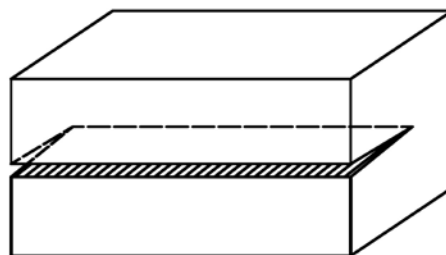


Figure 1. Cleavage cracking: nucleation parallel to the ice surface, and propagation in a plane parallel to the ice surface.

## EXPERIMENTAL DETAILS

The experimental test program was conducted at the Hamburg Ship Model Basin (HSVA).

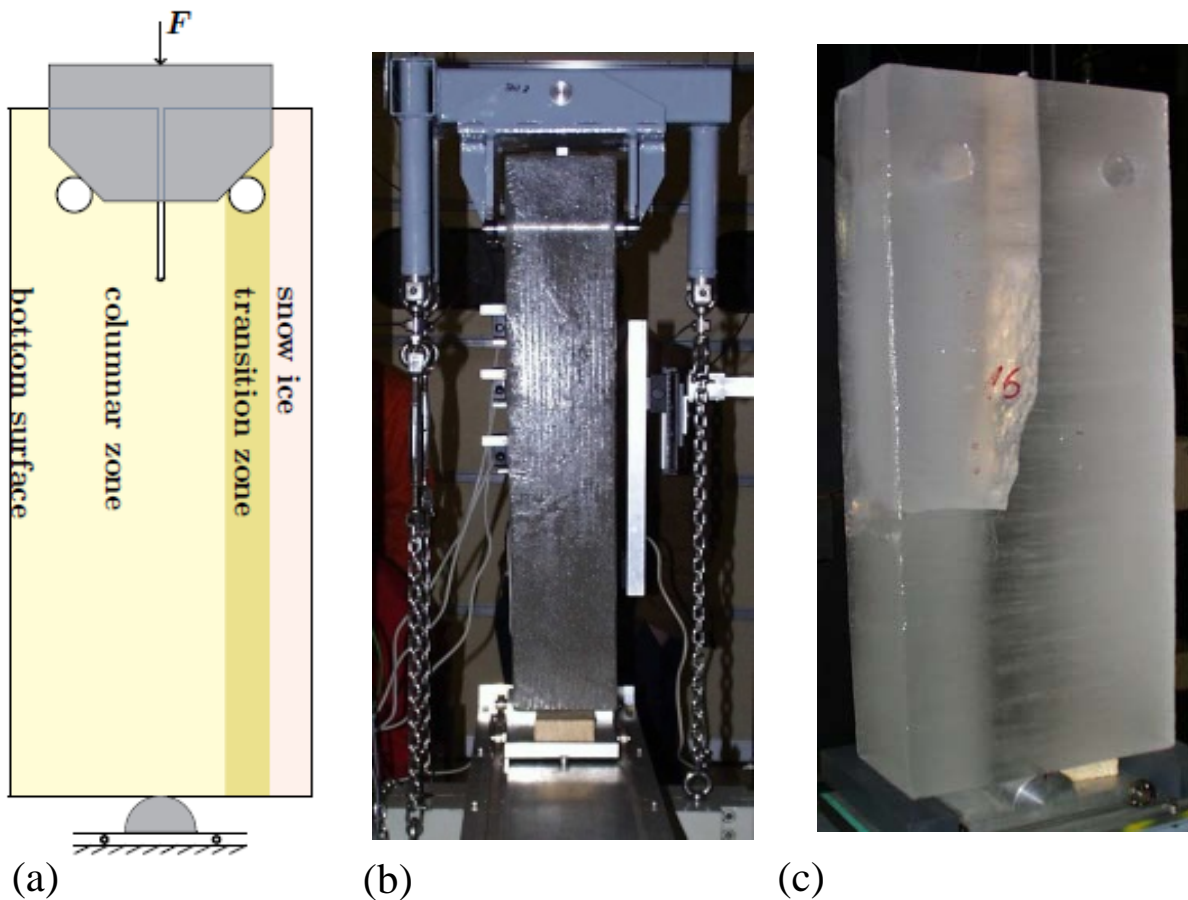


Figure 2. Wedge-loaded cleavage fracture test configuration: (a) test specimen symmetrically located on a solid half-cylinder of radius 40 mm, the front side of the crosshead showing the 45° angled surfaces that contact the ball bearings which are located on each end of the two pins (40 mm in diameter) that load the ice specimens; (b) side view of the test configuration; (c) angled view of test specimen 16.

The tests were conducted using a wedge-loaded compact tension configuration (Figure 2). Each wedge-loaded test specimen was supported symmetrically by a solid half-cylinder (Figure 2a), with the pins parallel to the long axis of the half-cylinder (Figure 2b). The tests were performed under closed-loop crosshead speed control. The crosshead consisted of two 45° wedge loading plates (Figure 2a), with each of the four contact surfaces resting on a ball bearing, which itself was attached to a cylindrical pin placed through-the-thickness of the test specimen. The pin diameters were 40 mm, the center-to-center distance between pins being 200 mm in all tests. Cracks were cut by a bandsaw and sharpened a little (a few mm) with a hacksaw blade. A cracked specimen is shown in Figure 2c.

The first set of wedge-loaded cleavage fracture tests was conducted during December 1999; average test temperature  $-3.1 \pm 0.5$  °C (Jochmann, 2001). During a March 1999 voyage by the German multi-purpose vessel *Neuwerk*, the ice for these 11 tests was harvested at the edge of

the land-fast and drift ice about 20 km northwest of the Norströmsgrund lighthouse, located near Luleå in the Gulf of Bothnia. The ice thickness at this location was about 0.42 m. Full thickness ice blocks approximately 1.2 m square were cut out, stored at  $-30^{\circ}\text{C}$ , and shipped to HSVA. The final test specimens were cut out by bandsaw. Three sensors were installed on the side of the specimen to measure crack-opening-displacements, while one was set to measure the crack-mouth-opening-displacement (Figure 3a).

The second set of cleavage fracture tests was conducted December 2, 2003; average test temperature  $-3^{\circ}\text{C}$  (Dempsey et al., 2004; Chapter 5, Mu, 2004). The ice for these 6 tests was harvested mid-April 2003 by Lennart Fransson's group from the middle of the Holfjärden Bay about 20 km from the Norströmsgrund lighthouse. A total of 9 full thickness  $0.4\text{ m} \times 1.0\text{ m} \times h_{\text{ice}}$  blocks were collected, with six of these being transported to HSVA, the remaining three being transported to Luleå University of Technology for uniaxial compressive and tensile strength tests. The ice thickness at this location was about 0.4m; this ice was harvested under very warm atmospheric conditions ( $+2$ ). The ice had a snow layer, a transition layer, and a columnar layer. Five laser sensors were attached to each test specimen at the locations indicated in Figure 3b.

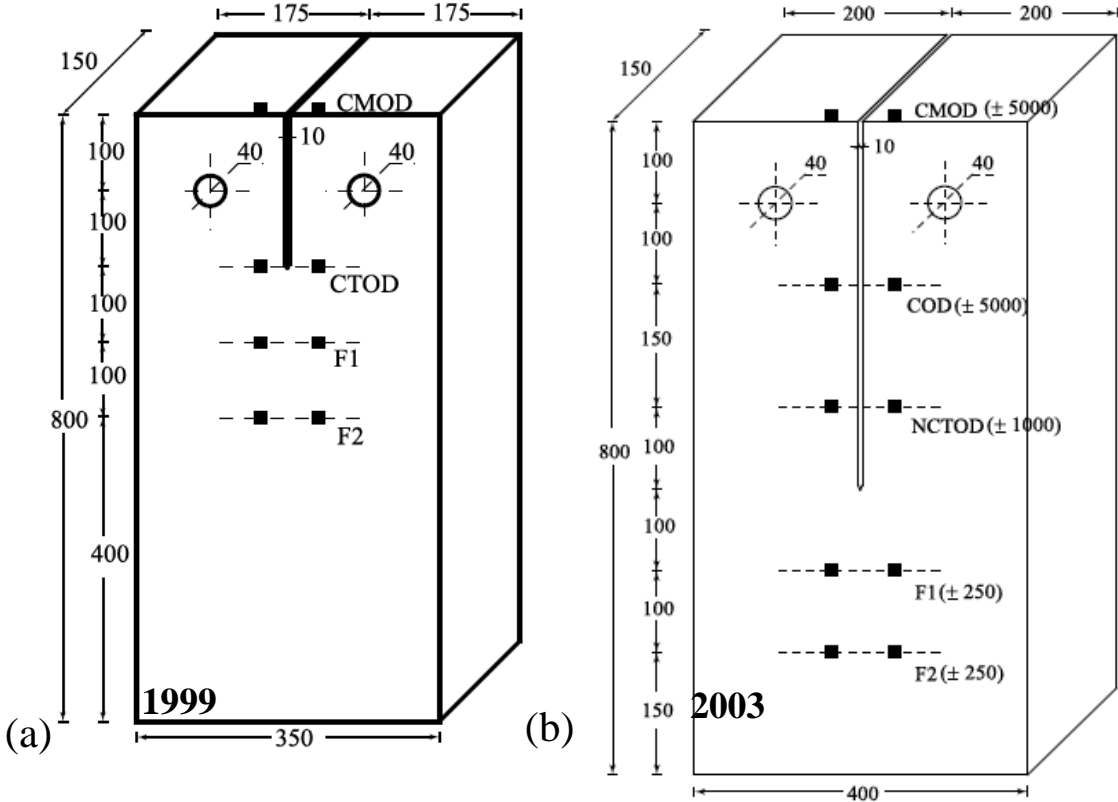


Figure 3. Representative configurations for the (a) 1999 and (b) 2003 wedge-loaded cleavage fracture tests. Dark squares identify sensor locations. Specimen dimensions are in mm while the crack-opening-displacement ranges (in parentheses) are in  $\mu\text{m}$ .

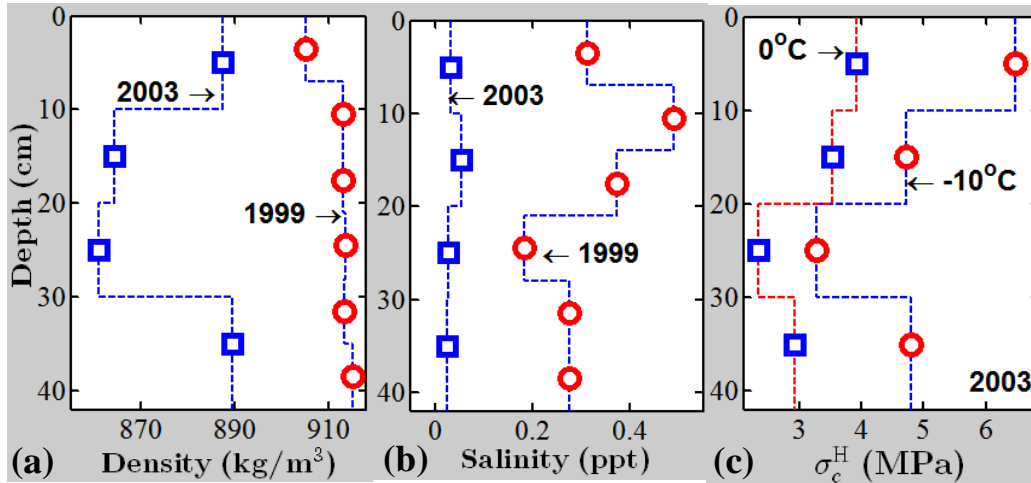


Figure 4. Density (a) and salinity (b) versus depth for the ice harvested in 1999 and 2003; (c) the horizontal compressive strength versus depth at  $-10^{\circ}\text{C}$  and  $0^{\circ}\text{C}$  for the 2003 ice, measured at a nominal strain rate of  $10^{-3} \text{ s}^{-1}$ .

### UNIAXIAL TENSILE AND COMPRESSIVE BEHAVIOR

The density and salinity profiles for both the 1999 and 2003 ice are shown in Figure 4. The horizontal compressive strength  $\sigma_c^H$  versus depth at  $-10^{\circ}\text{C}$  and  $0^{\circ}\text{C}$  for the 2003 ice is also shown in this figure (Figure 4c). Note that the lowest compressive strengths are in the middle portion of the ice sheet, and that test temperature has a significant influence. The test cylinders had a diameter of 70 mm. Horizontal and vertical thin sections of the 1999 and 2003 ice are shown in Figure 5. The 1999 and 2003 ice had an average grain size of  $8.1 \pm 0.8 \text{ mm}$  and  $4.3 \pm 0.3 \text{ mm}$ , respectively (given  $N$  grains within a plane area  $A$ ,  $d_{av} = \sqrt{4A/N\pi}$  as per Cole, 1986).

The compressive and tensile strength, versus strain rate, of the 1999 ice was measured (Weiss and Meyssonier, 2001). The uniaxial tensile tests were performed on dumbbell specimens with a cross section of  $50 \times 50 \text{ mm}^2$ , at  $-11^{\circ}\text{C}$ , with the tensile axis parallel to the growth direction of the ice, i.e. parallel to the columnar axis of the grains. The ice was taken from the central portion of the ice sheet. The uniaxial compression tests were performed on 70 mm cubes, with the compression axis perpendicular to the columnar axis (across-column compression). The ice was taken from different parts of the ice sheet. For both tension and compression, the tests were conducted under strain control, the strains (longitudinal and transverse) being measured by extensometers mounted on the ice samples. The tensile and compressive strengths, as well as the failure strains are shown in Figure 6.

An additional set of compressive and tensile tests were completed in 2003 (Fransson and Stenman, 2004). Vertical thin sections of the 2003 first-year sea ice showing grain structure variations within the depth of 40 cm depth are shown in Figure 7. Because of the very warm conditions at the time the ice was harvested, and because a long storage time preceded the tests, the 2003 ice had a rather low density (Figure 4a) and exceptionally low salinity (Figure 4b), caused by a plethora of large, drained, vertical brine channels. Several tests in the horizontal direction failed because of the presence of vertical macrocracks or large open brine channels (porosity estimated at 4.5%). The horizontal compressive strengths are plotted in Figure 4c. To ascertain the vertical compressive strengths, eight 70 mm diameter vertical cylinders were cored from the central portion of the 2003 ice blocks (depth 10 – 30 cm) and

tested in compression at the same strain rate as used for the horizontal compressive strength tests, viz.,  $10^{-3} \text{ s}^{-1}$ . The average density of this ice was  $876 \pm 3 \text{ kg/m}^3$ . The vertical compressive strength at  $-10^\circ\text{C}$  was  $\sigma_c^V = 4.37 \pm 1.26 \text{ MPa}$ , compared with  $\sigma_c^H = 3.27 \text{ MPa}$  at a depth of 25 cm (see Figure 4c). The compressive testing of the vertical cylinders resulted in extremely brittle catastrophic axial stability failures. Vertical and horizontal ice cylinders with a diameter of 70 mm were also tested in tension, at a loading rate of  $0.5 \text{ kNs}^{-1}$ . Again the ice tested came from the central 20 cm. For an average density of  $858 \pm 6 \text{ kg/m}^3$ , via 7 tests at  $-10^\circ\text{C}$ , it was found that  $\sigma_t^V = 1.31 \pm 0.47 \text{ MPa}$ , while for an average density of  $876 \pm 3 \text{ kg/m}^3$ , via 4 tests at  $-10^\circ\text{C}$ , it was found that  $\sigma_t^H = 1.36 \pm 0.81 \text{ MPa}$ .

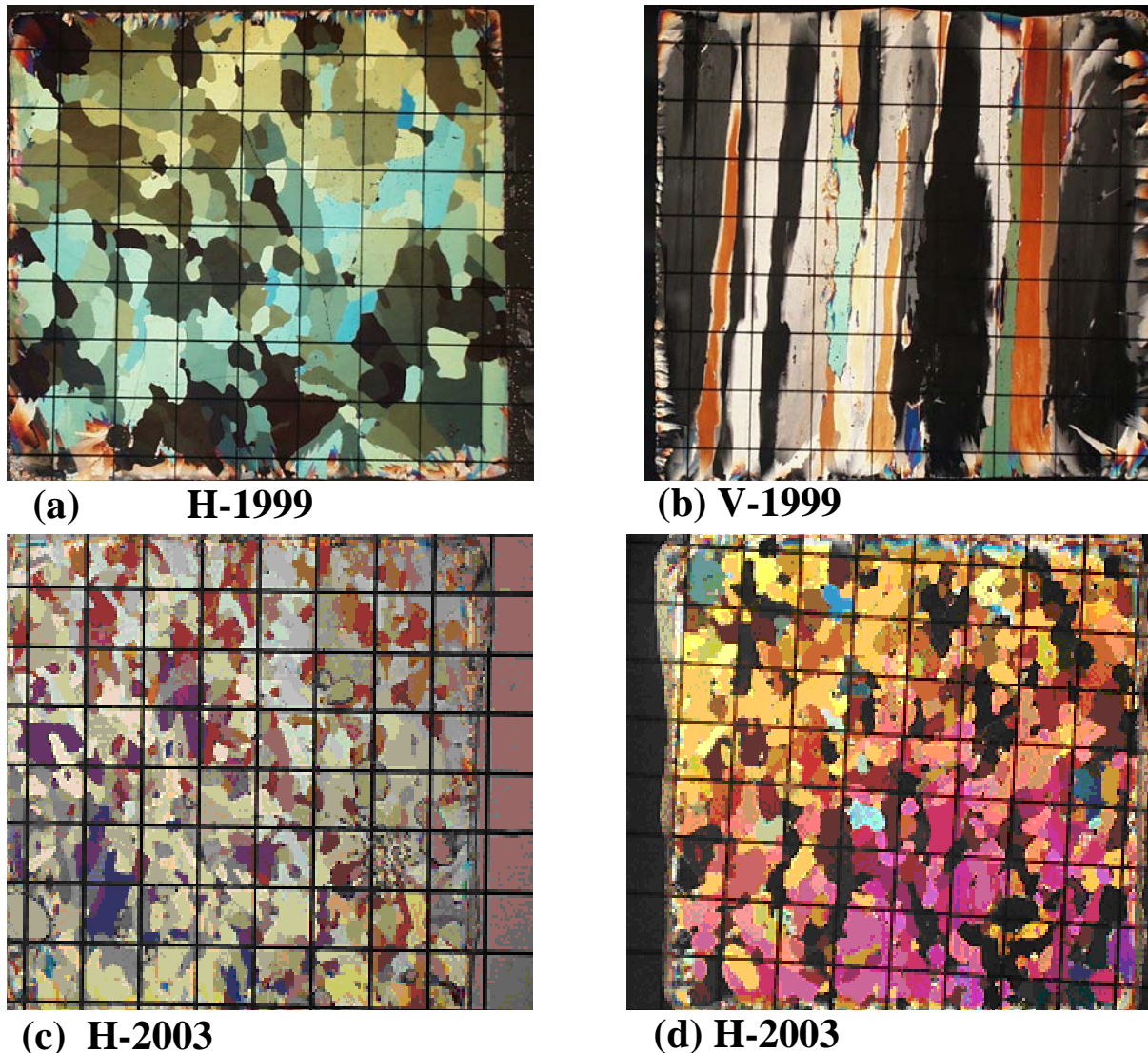


Figure 5. (a) horizontal, and (b) vertical thin section (1999); (c) and (d) horizontal thin sections (2003). The superimposed grid is 10 mm x 10 mm.

Regarding the tensile strengths and associated failure strains for the 1999 ice (shown in Figure 6), it is clear that no significant strain-rate effect was observed. The vertical strengths in this study are quite high ( $2.23 \pm 0.15 \text{ MPa}$ ); Kuehn et al. (1990) reported vertical tensile strengths of order 1 MPa for first-year sea ice. The very low salinity (0.2 ppt) and large grain size of the

1999 ice ( $8.1 \pm 0.8$  mm) are possible causes. In addition, the sample lateral dimension falls far short of the requisite 15-20 times the grain size (Schwarz et al., 1981, Richter-Menge and Jones, 1993). Uniaxial across-column compressive strengths and failure strains are also shown in Figure 6. A transition from macroscopic ductile (D) to macroscopic brittle (B) behavior is observed upon increasing the strain-rate from  $10^{-4}$  to  $10^{-3} \text{ s}^{-1}$ . It is not surprising that the tensile strength does not depend so much on the strain-rate, as strength is dictated by crack nucleation in this situation. Strain-rate effects are stronger for compressive strength, but the range explored here is too limited to see a significant effect. A brittle-to-ductile transition under compression between  $10^{-4}$  and  $10^{-3} \text{ s}^{-1}$  seems a bit larger than generally reported values ( $\sim 10^{-5}$  to  $10^{-4} \text{ s}^{-1}$ ), but this might be due to the characteristics of the ice (very low salinity).

Both vertical and horizontal strengths of the 2003 ice were studied using 70 mm diameter cylinders, with the smaller grain size of  $4.3 \pm 0.3$  mm, the diameter is of order 16 times the grain size. The ratio of the vertical to horizontal strengths is approximately 1.33, which is a bit lower than values observed by Kuehn and Schulson (1994) at  $-10^\circ\text{C}$  for saline ice. This again is no doubt because of the much lower salinity of the 2003 ice.

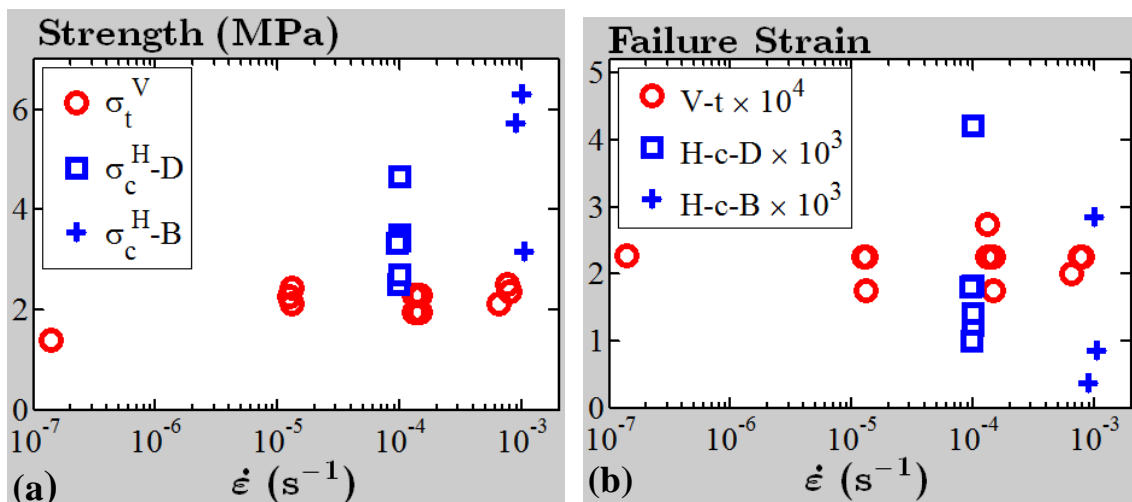


Figure 6. (a) Compressive (c) and tensile (t) strengths versus strain-rate for the ice tested in 1999, with the tensile (compressive) axis parallel (perpendicular) to the growth direction; (b) failure strain versus strain rate, with the tensile (compressive) strain measured in the columnar (across-column) direction. The growth direction is vertical (V), while the across-column direction is parallel to the plane of the ice sheet, which is horizontal (H). Failure under compression is either ductile (D) or brittle (B).

## CLEAVAGE FRACTURE TOUGHNESS

The wedge-loaded cleavage fracture test configuration was analysed by a finite element analysis, conducted using the ABAQUS/Standard package. The mesh was composed of eight-noded plane strain quadrilateral isoparametric elements; a refined mesh was employed in the vicinity of the crack tip, using triangular quarter-point elements. For each crack length, several  $J$  contours sweeping a path around the crack tip were calculated until the value of the  $J$  integral converged. The stress-intensity-factor was evaluated via  $K^2 = JE$ . Three different scenarios regarding the pin loading contact conditions were examined: (i) uniform bearing stresses applied over a  $45^\circ$  sector due to the undersized pin requirement (Newman, 1974); the

load approximated as a point load; (iii) the pin modelled as a rigid inclusion (in some tests the pins were frozen-in by wetting the pins first). It was observed that the cracks propagated straight ahead only if the pins were loose. If they were frozen-in, the cracks curved slowly as they propagated (always in the same direction).

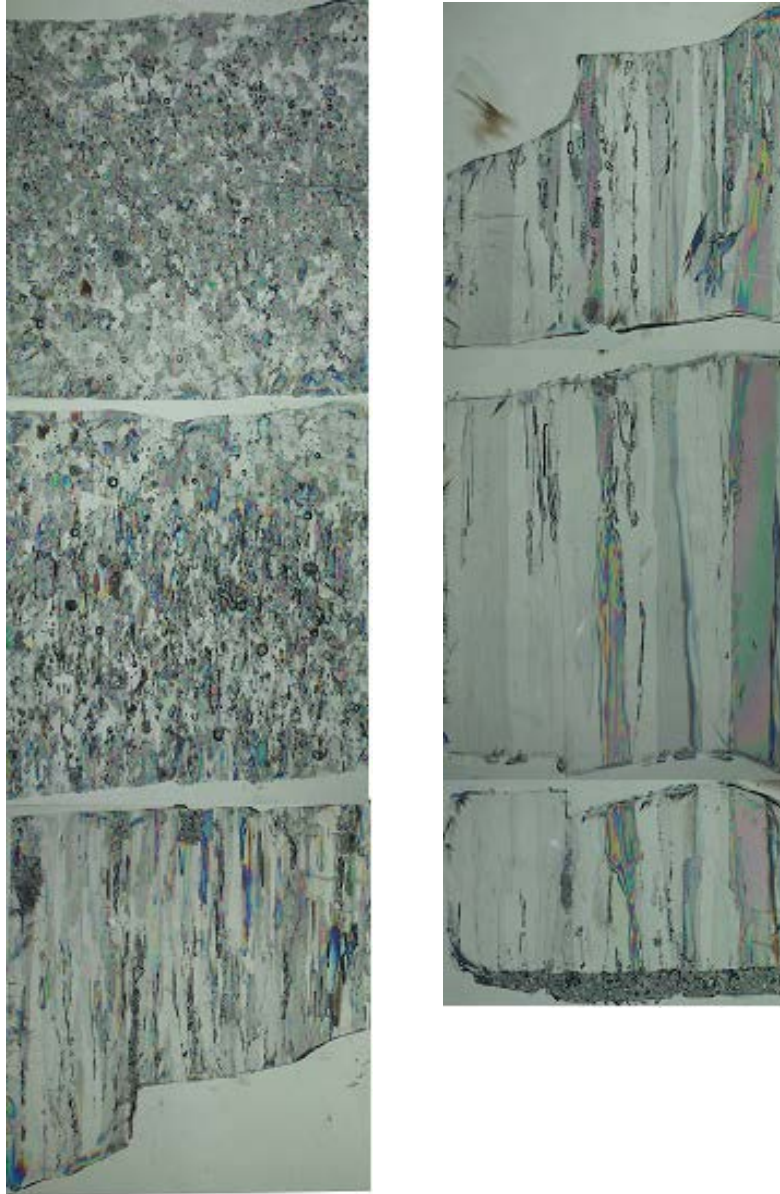


Figure 7. Vertical thin sections of the 2003 first-year sea ice spanning the depth of 40 cm.

The wedge-loading induces a crack-parallel compression, which serves to stabilize the crack path. With the pins frozen, and the ball bearings not working perfectly, the crack-parallel compression on either side of the crack differed slightly; the crack was thus loaded in mixed-mode. While negligible, the Mode II component was sufficient to cause the crack to curve smoothly as it propagated (and always to the same side).

The fabricated cracks in the 1999 cleavage splitting tests encountered columnar grained ice, the long axes parallel to the growth direction, with the crystallographic c-axes confined

essentially to the horizontal plane, which was the plane of crack extension in these tests (Figure 8a). The fabricated crack lengths were  $25d_{av}$ , while the crack front spanned  $19d_{av}$ . The across-column uniaxial and biaxial compression loading of columnar freshwater ice crystals was studied by Gupta et al. (1997); under certain conditions cracks were observed to *split* the columnar grains. The nucleation of these *splitting cracks* (called here cleavage cracks) was studied. It was concluded that damage must be initiated via in-plane and out-of-plane sliding of grain facets in the column axis direction, and that this must necessarily precede cleavage across the grains. The damage being comprised of local decohesion pockets distributed along grain boundaries and at triple junctions in the vicinity of the crack front.

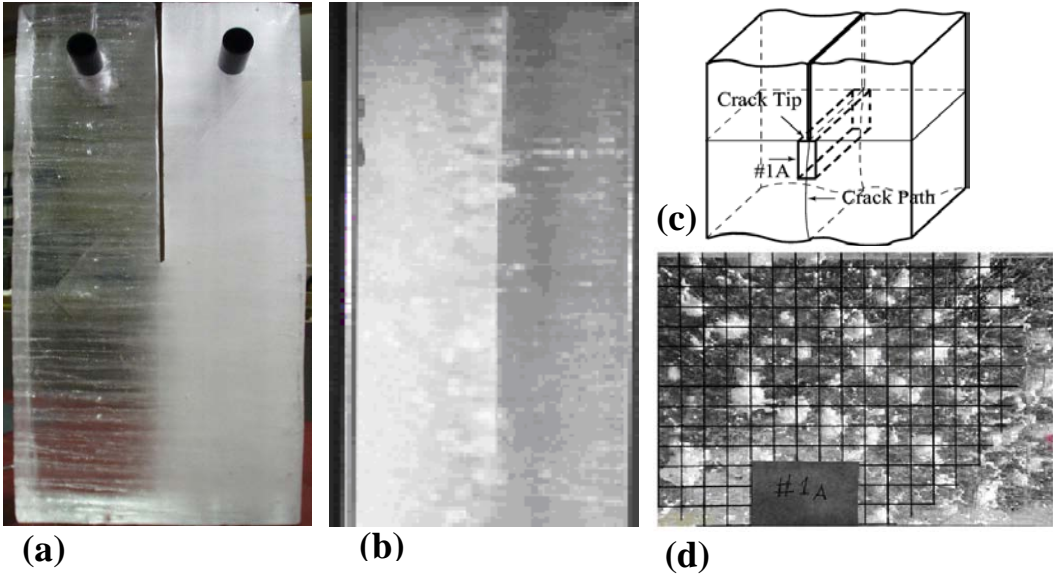


Figure 8. Ice samples tested in (a) 1999, (b) 2003; (c) drawing showing the site where the backlit thick section in (d) was cut out.

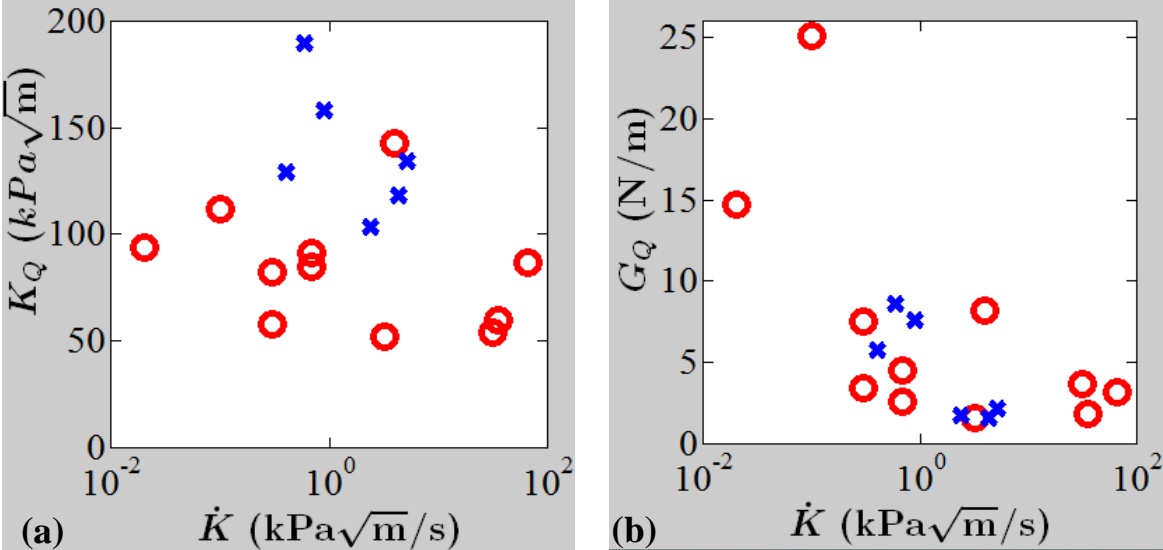


Figure 9. The 1999 (o) and 2003 (x) cleavage splitting tests: (a) apparent fracture toughness  $K_Q$ , and (b) apparent fracture energy  $G_Q$ , versus loading rate.

The ice in the 2003 fracture tests was quite different, having large drained brine channels present Figure 8b. The fabricated crack lengths were  $105d_{av}$ , while the crack front spanned  $47d_{av}$ . Sections a half-inch thick, cut out of either side of the crack on the crack path, were fabricated (Figure 8c); a backlit photo of one of these sections is shown in Figure 8d. The drained brine channels had become filled by frozen condensation and moisture.

The apparent fracture toughness  $K_Q$  (Dempsey, 1991) values obtained for a range of loading rates are shown in Figure 9, as are the apparent fracture energies  $G_Q=C(t) K_Q^2$  in which  $C(t)$  is the creep compliance. Note that the 2003 test samples were much larger relative to the grain size, and the crack lengths were also much longer, and hence the tests were more notch sensitive. The cleavage fracture toughness values plotted in Figure 9a are similar in magnitude to those reported by Matsushita et al. (2000). More data is needed at the higher loading rates. Tentatively, there is a decrease in the cleavage fracture toughness with loading rate. The role played by the indentation velocity is in all likelihood linked to this behaviour.

## SUMMARY

In this paper, the fracture energy associated with the crack growth initiation of macrocracks propagating in a plane that is parallel to the ice surface has been measured. The tensile and compressive strengths, and failure strains, of the ice in the cleavage zone of tensile cracking have been measured also. As little is known about the actual micromechanics of across-column cracking, the paper has minimal discussion regarding size effects or scaling.

## ACKNOWLEDGEMENTS

This research was supported by two projects, the “Validation of Low Level Ice Forces on Coastal Structures (LOLEIF)”, an EU MAST III Project, and “Measurements on Structures in Ice (STRICE)”, an EU FP5 EESD Project. In addition, the first author (J.P.D.) acknowledges the research support of the U.S. National Science Foundation (ANT-0338226).

## REFERENCES

- ABAQUS/Standard Version 6.2, 2000. User Manual. Hibbert, Karlsson and Sorenson, Pawtucket, USA.
- Cole, D.M., 1986. Effect of grain size on the internal fracturing of polycrystalline ice. CRREL Report 86-5.
- Dempsey, J.P., 1991. The fracture toughness of ice. In: Jones, S.P., McKenna, R.F., Tillotson, J., Jordaan, I.J., Eds., Ice-Structure Interaction, Berlin:Springer-Verlag, p.109-145.
- Dempsey, J.P., Mu, Z., Jochmann, P., Palmer, A.C., 2004. Cleavage fracture toughness of warm brackish ice, STRICE Report 5.5.1.
- Evans, A.G., Palmer, A.C., Goodman, D.J., Hutchinson, J.W., Ponter, A.R.S., Williams, G.J., 1984. Indentation spalling of edge-loaded ice sheets. Proceedings of the 7<sup>th</sup> International IAHR Ice Symposium, 113-121.
- Fransson, L., Stenman, U., 2004. Mechanical properties of ice at Norströmsgrund, Test 2003. STRICE Report D-4.3.3.
- Gupta, V., Picu, R.C., Bergström, J.S., 1997. Nucleation of splitting cracks in columnar freshwater ice, Acta Materialia, vol. 45, p. 1411-1423.
- Jochmann, P., 2001. Fracture toughness laboratory tests. Data Report. LOLEIF Report 5B.
- Kamio, Z., Matsushita, H., Strnadel, B., 2003. Statistical analysis of ice fracture characteristics. Engineering Fracture mechanics, vol. 70, p. 2075-2088.

- Kärnä, T., Järvinen, E., 1999. Symmetric and asymmetric flaking processes. Proceedings of the 15th International POAC Conference, Vol. 3, p. 988-1000.
- Kuehn, G.A., Lee, R.W., Nixon, W.A., Schulson, E.M., 1990. The structure and tensile behaviour of first-year sea ice and laboratory-grown saline ice, *Journal of Offshore Mechanics and Arctic Engineering*, vol. 112, p.357-363.
- Kuehn, G.A., Schulson, E.M., 1994. The mechanical properties of saline ice under uniaxial compression, *Annals of Glaciology*, vol. 19, p. 39-48.
- Matsushita, H., Kamio, Z., Sakai, M., Takeuchi, T., Terashima, T., Akagawa, S., Nakazawa, N., Saeki, H., 2000. Consideration of the failure mode of an ice sheet, Proceedings of the 10<sup>th</sup> ISOPE Conference, 577-582.
- Matsushita, H., Kamio, Z., Ushikoshi, J., Sakai, M., Takeuchi, T., Terashima, T., Akagawa, S., Nakazawa, N., Saeki, H., 2001. Failure mode of an ice sheet-cracking, Proceedings of the 11<sup>th</sup> ISOPE Conference, 707-712.
- Mu, Z., 2004. Fracture of Baltic and Antarctic First-Year Sea Ice. Ph.D. Thesis, Clarkson University.
- Newman, J.C. Jr., 1974. Stress analysis of the compact specimen including the effects of pin loading. *Fracture Analysis*, ASTM STP 560, p.105-121.
- Parsons, B.L., Snellen, J.B., Hill, B., 1986. Physical modeling and the fracture toughness of sea ice. Proceedings of the 5<sup>th</sup> International OMAE Conference, Vol. IV, 358-364.
- Richter-Menge, J.A., Jones, K.F., 1993. The tensile strength of first-year sea ice. *Journal of Glaciology*, vol. 39, p.609-618.
- Schwarz, J., Hirayama, K.I., Wu, H.C., 1974. Effect of ice thickness on ice forces. *Offshore Technology Conference*, OTC-2048.
- Schwarz, J., Frederking, R., Gavrillo, V., Petrov, I.G., Hirayama, K.-I., Mellor, M., Tryde, P., Vaudrey, K.D., 1981. Standardized testing methods for measuring mechanical properties of ice, *Cold Regions Science and Technology*, vol. 4, p. 245-253.
- Weiss, J., Meyssonier, J., 2001. Micro mechanics. LOLEIF Report No. 7.